



Slow Crack Growth of Brittle Materials With Exponential Crack-Velocity Formulation— Part 2: Constant Stress Rate Experiments

Sung R. Choi
Ohio Aerospace Institute, Brook Park, Ohio

Noel N. Nemeth and John P. Gyekenyesi
Glenn Research Center, Cleveland, Ohio

The NASA STI Program Office . . . in Profile

Since its founding, NASA has been dedicated to the advancement of aeronautics and space science. The NASA Scientific and Technical Information (STI) Program Office plays a key part in helping NASA maintain this important role.

The NASA STI Program Office is operated by Langley Research Center, the Lead Center for NASA's scientific and technical information. The NASA STI Program Office provides access to the NASA STI Database, the largest collection of aeronautical and space science STI in the world. The Program Office is also NASA's institutional mechanism for disseminating the results of its research and development activities. These results are published by NASA in the NASA STI Report Series, which includes the following report types:

- **TECHNICAL PUBLICATION.** Reports of completed research or a major significant phase of research that present the results of NASA programs and include extensive data or theoretical analysis. Includes compilations of significant scientific and technical data and information deemed to be of continuing reference value. NASA's counterpart of peer-reviewed formal professional papers but has less stringent limitations on manuscript length and extent of graphic presentations.
- **TECHNICAL MEMORANDUM.** Scientific and technical findings that are preliminary or of specialized interest, e.g., quick release reports, working papers, and bibliographies that contain minimal annotation. Does not contain extensive analysis.
- **CONTRACTOR REPORT.** Scientific and technical findings by NASA-sponsored contractors and grantees.

- **CONFERENCE PUBLICATION.** Collected papers from scientific and technical conferences, symposia, seminars, or other meetings sponsored or cosponsored by NASA.
- **SPECIAL PUBLICATION.** Scientific, technical, or historical information from NASA programs, projects, and missions, often concerned with subjects having substantial public interest.
- **TECHNICAL TRANSLATION.** English-language translations of foreign scientific and technical material pertinent to NASA's mission.

Specialized services that complement the STI Program Office's diverse offerings include creating custom thesauri, building customized data bases, organizing and publishing research results . . . even providing videos.

For more information about the NASA STI Program Office, see the following:

- Access the NASA STI Program Home Page at <http://www.sti.nasa.gov>
- E-mail your question via the Internet to help@sti.nasa.gov
- Fax your question to the NASA Access Help Desk at 301-621-0134
- Telephone the NASA Access Help Desk at 301-621-0390
- Write to:
NASA Access Help Desk
NASA Center for Aerospace Information
7121 Standard Drive
Hanover, MD 21076



Slow Crack Growth of Brittle Materials With Exponential Crack-Velocity Formulation— Part 2: Constant Stress Rate Experiments

Sung R. Choi
Ohio Aerospace Institute, Brook Park, Ohio

Noel N. Nemeth and John P. Gyekenyesi
Glenn Research Center, Cleveland, Ohio

National Aeronautics and
Space Administration

Glenn Research Center

Acknowledgments

The authors are thankful to R. Pawlik for experimental work.

This report is a formal draft or working paper, intended to solicit comments and ideas from a technical peer group.

The Aerospace Propulsion and Power Program at NASA Glenn Research Center sponsored this work.

Available from

NASA Center for Aerospace Information
7121 Standard Drive
Hanover, MD 21076

National Technical Information Service
5285 Port Royal Road
Springfield, VA 22100

Available electronically at <http://gltrs.grc.nasa.gov/GLTRS>

Slow Crack Growth of Brittle Materials With Exponential Crack-Velocity Formulation—Part 2: Constant Stress Rate Experiments

Sung R. Choi
Ohio Aerospace Institute
Brook Park, Ohio 44142

Noel N. Nemeth and John P. Gyekenyesi
National Aeronautics and Space Administration
Glenn Research Center
Cleveland, Ohio 44135

Summary

The previously determined life prediction analysis based on an exponential crack-velocity formulation was examined using a variety of experimental data on glass and advanced structural ceramics in constant stress rate and preload testing at ambient and elevated temperatures. The data fit to the relation of strength versus the log of the stress rate was very reasonable for most of the materials. Also, the preloading technique was determined equally applicable to the case of slow-crack-growth (SCG) parameter $n > 30$ for both the power-law and exponential formulations. The major limitation in the exponential crack-velocity formulation, however, was that the inert strength of a material must be known a priori to evaluate the important SCG parameter n , a significant drawback as compared with the conventional power-law crack-velocity formulation.

Introduction

Advanced ceramics are candidate materials for structural applications in advanced heat engines and heat recovery systems. The major limitation of these materials in hostile environments is slow-crack-growth (SCG)-associated failure where slow growth of inherent microcracks, defects, or flaws can take place until a critical size for catastrophic failure is reached. To ensure accurate life prediction of ceramic components, it is important to accurately evaluate SCG or life prediction parameters of a material under specified loading and environmental conditions.

Life prediction (or SCG) parameters of a material depend on what type of crack-velocity formulation is used to determine them. The power-law crack-velocity formulation has been exclusively used for several decades to describe the slow-crack-growth behavior of a variety of brittle materials including glasses, glass ceramics, and advanced structural ceramics at ambient and elevated temperatures. The notable advantage of the power-law formulation over other crack-velocity formulations is its mathematical simplicity in life-prediction-related analysis. It has also been observed that the power-law formulation has adequately described the slow-crack-growth behavior of many brittle materials. Because of these merits, the power-law formulation has been used in two recent ASTM test standards (refs. 1 and 2) to determine SCG parameters of advanced ceramics in constant stress rate testing at both ambient and elevated temperatures. Alternative crack-velocity formulations take exponential forms to account for the influence of other phenomena (such as a corrosion reaction, diffusion control, thermal activation, etc.). However, these exponential forms do not give simple mathematical expressions of life prediction formulations, though the forms might better represent the actual SCG behavior of some materials. Because of this mathematical inconvenience, the exponential crack-velocity formulation has rarely been used for brittle materials as a means of life prediction methodology in testing or analysis.

In part 1 of this report (ref. 3), the exponential crack-velocity formulation was used to achieve a more convenient and simplified life prediction analysis using three widely utilized load configurations of constant stress rate (dynamic fatigue), constant stress (static fatigue), and cyclic stress (cyclic fatigue). The resulting analysis was compared with that of the power-law formulation to determine which formulation would yield a better life prediction methodology in terms of accuracy and convenience. This report, emphasizing experimental aspects and verifications, will describe in more detail the exponential formulation with reference to the conventional power-law formulation. A variety of experimental data, determined in constant stress rate and preload testing for glasses and advanced structural ceramics at both ambient and elevated temperatures, will be used for this purpose.

All symbols used in this report are listed in the appendix.

This work was sponsored in part by the HOT/PC and ZCET projects at the NASA Glenn Research Center, Cleveland, Ohio.

Theoretical Background

The results of the previous SCG analysis (ref. 3) using the exponential crack-velocity formulation will be briefly presented in this section for the case of constant stress rate loading. The companion SCG analysis using the conventional power-law crack velocity will also be included for the purpose of comparison and generalization of the analysis.

Power-Law SCG Formulation

The widely utilized conventional power-law crack velocity above the fatigue limit is expressed in the following familiar form:

$$v = \frac{da}{dt} = A \left(\frac{K_I}{K_{IC}} \right)^n \quad (1)$$

where

| | |
|----------|---|
| v | crack velocity |
| a | crack size |
| t | time |
| K_I | mode I stress intensity factor |
| K_{IC} | mode I critical stress intensity factor (or fracture toughness) |
| A, n | material- and environment-dependent SCG parameters |

Typically, SCG testing to determine related SCG parameters is performed by applying constant stress rate, constant stress, or cyclic stress loading to machined test specimens. Constant stress rate testing determines strength as a function of applied stress rate whereas constant stress and cyclic stress testing measure time to failure as a function of applied stress. The strength as a function of applied stress rate in constant stress rate loading can be analytically derived to give the following familiar relation (refs. 4 and 5):

$$\sigma_f = D\dot{\sigma}^{1/n+1} \quad (2)$$

where σ_f is the fracture stress corresponding to the applied stress rate $\dot{\sigma}$. The parameter D can be expressed as (refs. 1, 2, and 5)

$$D = \left[B(n+1)S_i^{n-2} \right]^{1/n+1} \quad (3)$$

where S_i is the inert strength whereby no slow crack growth occurs, and $B = 2K_{IC}/[AY^2(n-2)]$ where Y is the crack geometry factor in the relation of $K_I = Y\sigma a^{1/2}$ with σ as remote applied stress. The SCG parameters n and D (and B or A) can be obtained by a linear regression analysis of $\log \sigma_f$ versus $\log \dot{\sigma}$ with experimental data in conjunction with equation (2). Hence, it is straightforward to determine SCG parameters n and D by least-squares fitting of the data, which is the most advantageous feature in the power-law crack-velocity formulation. This convenience and merit in mathematical simplicity in addition to the use of routine test techniques have led for several decades to the almost exclusive use of the power-law crack-velocity formulation in life prediction analysis and testing for many brittle materials over a wide range of temperatures.

Exponential SCG Formulation

Several different exponential crack velocity forms that have been proposed consider other influences on the SCG mechanism. These include a chemically assisted corrosion reaction (ref. 6), diffusion control (ref. 7), a thermally activated process (ref. 8), a chemical reaction with constant crack-tip configuration (ref. 9), kinetic crack growth (ref. 10), and others (ref. 11). Taking these other factors into consideration, the following generalized exponential crack velocity forms have thus been proposed:

$$v = A \exp \left[n \left(\frac{K_I}{K_{IC}} \right) \right] \quad (4)$$

$$v = A \left(\frac{K_I}{K_{IC}} \right) \exp \left[n \left(\frac{K_I}{K_{IC}} \right) \right] \quad (5)$$

$$v = A \left(\frac{K_{IC}}{K_I} \right) \exp \left[n \left(\frac{K_I}{K_{IC}} \right) \right] \quad (6)$$

$$v = A \exp \left[n \left(\frac{K_I}{K_{IC}} \right)^2 \right] \quad (7)$$

$$v = A \left(\frac{K_I}{K_{IC}} \right) \exp \left[n \left(\frac{K_I}{K_{IC}} \right)^2 \right] \quad (8)$$

where A and n are SCG parameters and are different from those used in the power-law formulation. Unlike the power-law crack-velocity formulation, none of the above exponential crack-velocity forms yield simple, analytical expressions for either the resulting strength as a function of applied stress rate under constant stress rate loading or the resulting time to failure as a function of applied stress in either constant stress or cyclic stress loading. Several attempts have been made under constant stress rate and constant stress loading to obtain corresponding lifetime expressions through numerical integration incorporating linear (refs. 12 and 13) or nonlinear (ref. 14) regression analysis. However, this approach still involves complexity in regression technique as compared with the simple least-squares approach routinely used in the power-law formulation.

Slow-crack-growth analyses of three load configurations of constant stress rate, constant stress, and cyclic stress were made in part 1 of this report (ref. 3) to obtain simpler formulations through numerical approaches. Little difference in SCG formulation existed among equations (4) through (6), and equation (4) was regarded as a representative exponential crack-velocity form. Hence, equation (4) was used exclusively in the previous analysis. To minimize the number of variables to be specified (such as A , a , σ , S_i , K_{IC} , and t) in the analysis it was convenient to use a normalized scheme, as used previously for the power-law velocity formulation (refs. 15 and 16):

$$K^* = \frac{K_I}{K_{IC}}; \quad T^* = \frac{A}{a_i} t; \quad C^* = \frac{a}{a_i}; \quad \sigma^* = \frac{\sigma}{S_i}; \quad \dot{\sigma}^* = \frac{\dot{\sigma}}{T^*} \quad (9)$$

where

| | |
|------------------|-------------------------------|
| K^* | stress intensity factor (SIF) |
| T^* | time |
| C^* | crack size |
| σ^* | applied stress |
| $\dot{\sigma}^*$ | applied stress rate |

and a_i is the critical crack size in the inert condition or is the initial crack size. Using these variables, the exponential crack-velocity form (eq. (4)) was normalized as follows:

$$\frac{dC^*}{dT^*} = e^{nK^*} \quad (10)$$

The corresponding normalized SIF K^* in constant stress rate loading is

$$K^* = \dot{\sigma}^* T^* (C^*)^{1/2} \quad (11)$$

As is typical of ceramics, the crack size at instability either in an inert or fatigue environment was assumed to be small as compared with the body of the specimens or components (i.e., an infinite-body assumption). Equation (10) was solved numerically using a fourth-order Runge-Kutta method. The initial condition was $C^* = 1.0$ at $T^* = 0$, and the instability condition was $K^* = 1.0$ and $dK^*/dC^* > 0$.

The results of numerical solution of normalized strength σ_f^* as a function of normalized stress rate $\dot{\sigma}^*$ showed that a linear relationship between σ_f^* and $\ln \dot{\sigma}^*$ holds for most values of n from 10 to 100 within the range $\sigma_f^* = 0.2$ to 0.9 with correlation coefficients $r^2 > 0.9970$ (see fig. 1). A linear regression analysis of σ_f^* and $\ln \dot{\sigma}^*$ in the range of $\sigma_f^* = 0.2$ to 0.9 was obtained as follows:

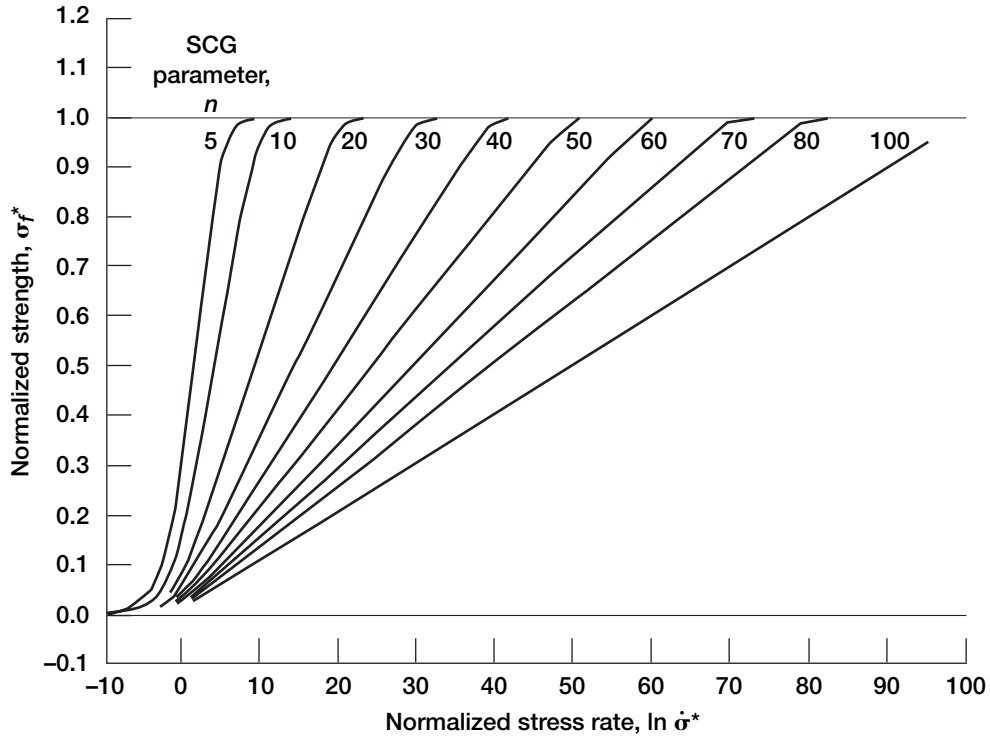


Figure 1.—Numerical solution of normalized strength σ_f^* as function of normalized stress rate $\dot{\sigma}^*$ at different values of SCG parameter n using exponential crack-velocity formulation. Determined previously in reference 3.

$$\sigma_f^* = \frac{1}{n'} \ln \dot{\sigma}^* + \beta \quad (12)$$

where $1/n'$ and β are the slope and intercept for a given n value, respectively. A relationship between the true n (an input datum) and the apparent (calculated) n' for $n \geq 10$ was found:

$$n' = 0.9775n + 1.7384 \quad (13)$$

with a correlation coefficient of $r^2 = 0.9995$. Since the difference between n' and n was ≥ 8 percent for $n \leq 10$ and ≤ 3 percent for $n \geq 20$, a further approximation of equation (13) could be made for $n \geq 20$:

$$n' \approx n \quad (14)$$

The relationship between the intercept β and n was

$$\beta = 2.666(n)^{-1.279} \quad (15)$$

with a correlation coefficient of $r^2 = 0.9973$. For a nonnormalized expression, equation (9) was used to reduce equation (12) to

$$\frac{\sigma_f}{S_i} = \frac{1}{n'} \ln \dot{\sigma} + \chi \quad (16)$$

or

$$\sigma_f = \frac{1}{n'} \ln \dot{\sigma} + S_i \chi \quad (17)$$

where

$$\chi = \frac{1}{n'} \ln \left(\frac{a_i}{AS_i} \right) + \beta \quad (18)$$

The SCG parameters n' and χ in constant stress rate loading were obtained from the slope and intercept by a linear regression analysis of σ_f or σ_f/S_i versus $\ln \dot{\sigma}$ based on equation (16) or (17). With n' thus determined, the true SCG parameter n could be evaluated from equation (13) or (14). The SCG parameter A was determined from equation (18) together with the associated parameters. For the case of $\sigma_f^* \geq 0.4$, β in equation (15) was insignificant compared with σ_f^* , with a maximum of about 7 percent at $n = 20$ and decreasing as $n > 20$, thereby being reduced to

$$\beta \approx 0 \quad (19)$$

which results in $\chi \approx [\ln (a_i/AS_i)]/n$. Likewise, in this case $n' \approx n$ (eq. (14)).

A distinct difference in functional expression between the power-law and exponential SCG formulations is that in the power-law formulation, $\log \sigma_f$ is plotted as a function of $\log \dot{\sigma}$, whereas in the exponential formulation, σ_f/S_i is plotted as a function of $\ln \dot{\sigma}$. As a result, the knowledge of inert strength of a material is a prerequisite in determining n in the exponential formulation (see eq. (16) or (17)), which is not the case in the power-law formulation.

Experimental Verification and Discussion

The experimental data determined previously in constant stress rate testing for various brittle materials at both ambient and elevated temperatures will be utilized to verify the exponential SCG analysis. The constant stress rate data have been accumulated at NASA Glenn over more than a decade from a variety of brittle materials including glasses, glass ceramics, and advanced ceramics such as aluminas (Al_2O_3), silicon carbides (SiC), and both monolithic and SiC whisker-reinforced silicon nitrides (Si_3N_4). Preloading data determined for alumina in constant stress rate testing at elevated temperature will also be used to examine the appropriateness of the exponential crack-velocity form.

Constant Stress Rate Testing Data

The strength as a function of stress rate determined for three brittle materials of glass, alumina, and glass ceramic (refs. 17 to 20) that have exhibited SCG behavior even in ambient-temperature distilled water is shown in figure 2, where σ_f was plotted against $\ln \dot{\sigma}$ based on the exponential formulation of equation (17). The strength decreases with decreasing stress rate, indicative of SCG susceptibility, yielding a reasonably good linearity in the relation σ_f versus $\ln \dot{\sigma}$. The individual SCG parameters n

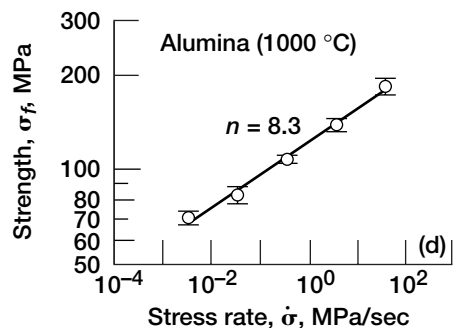
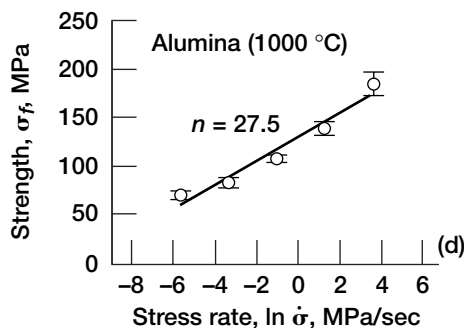
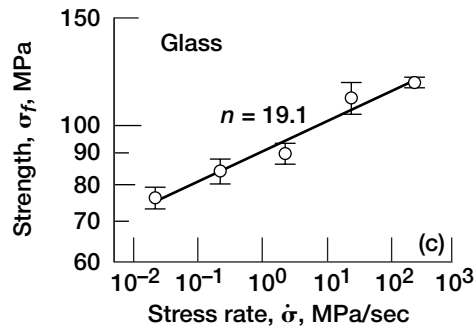
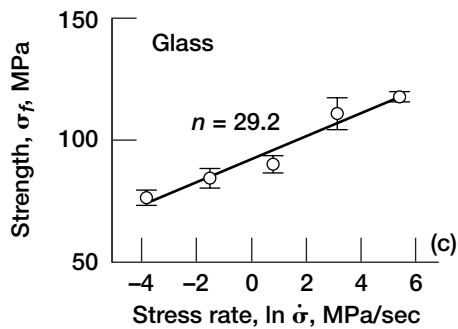
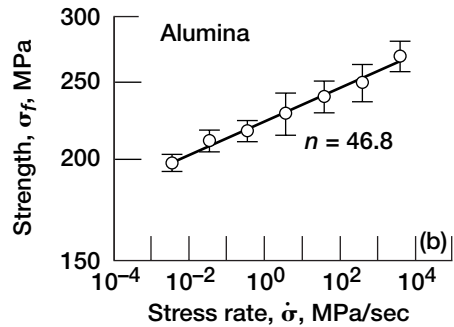
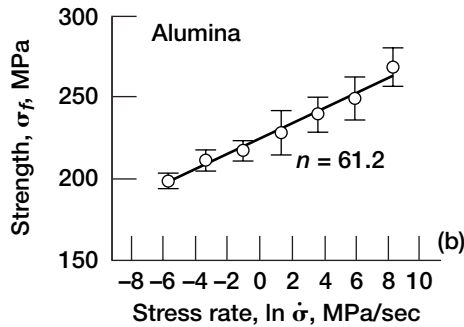
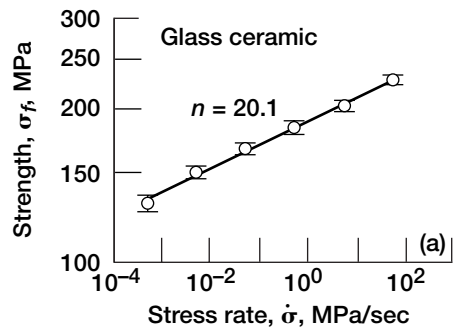
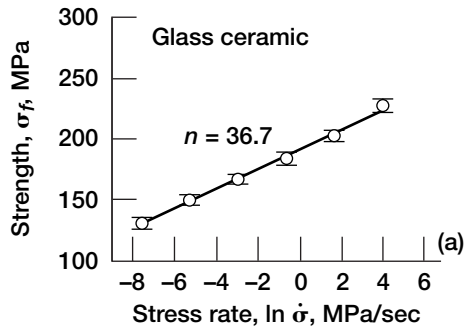


Figure 2.—Strength σ_f as function of stress rate $\dot{\sigma}$ in exponential crack-velocity formulation using equation (17) under constant stress rate loading. (a) Glass ceramic Pyroceram (Corning, Corning, NY) in ambient distilled water for SCG parameter $n = 36.7$. (b) 96-wt% alumina in ambient distilled water for $n = 61.2$. (c) Indented and annealed soda-lime glass in ambient distilled water for $n = 29.2$. (d) 96-wt% alumina at 1000 °C in air for $n = 27.5$.

Figure 3.—Strength σ_f as function of stress rate $\dot{\sigma}$ in power-law crack-velocity formulation using equation (2) under constant stress rate loading. (a) Glass ceramic Pyroceram in ambient distilled water for SCG parameter $n = 20.1$. (b) 96-wt% alumina in ambient distilled water for $n = 46.8$. (c) Indented and annealed soda-lime glass in ambient distilled water for $n = 19.1$. (d) 96-wt% alumina at 1000 °C in air for $n = 8.3$.

and χ were determined from the slope and intercept by a linear regression analysis of σ_f versus $\ln \dot{\sigma}$ using equation (17) together with the inert strength of each material. The resulting SCG parameters and the correlation coefficient in regression analysis for each material are shown in table I. Figure 3 is the power-law counterpart of figure 2 with plots of σ_f as a function of $\dot{\sigma}$ taken from equation (2). Note that the σ_f and $\dot{\sigma}$ scales are logarithmic. A comparison of figures 2 and 3 reveals no significant difference in data fit between the exponential and power-law formulations. Both cases yield very reasonable values of correlation coefficients. However, the overall data fit^a seems to be slightly better for the power-law than for the exponential formulation in view of their respective correlation coefficients, particularly for the elevated-temperature 96-wt% alumina data (see figs. 2(d) and 3(d)).

The elevated-temperature strength as a function of stress rate for a variety of advanced ceramics, including aluminas, silicon nitrides, and silicon carbides (ref. 22), is summarized in figure 4, where σ_f^* was plotted as a function of $\dot{\sigma}$ based on equation (16). Similar to the results in figure 2, the strength degradation with decreasing stress rate was evident for each material with the degree depending on the type of material tested. A reasonable linearity is found between σ_f^*/S_i and $\ln \dot{\sigma}$. The SCG parameters determined by the linear regression analysis based on equation (16) are also shown in table I together with those evaluated for the power-law formulation. Figure 5 is the power-law counterpart of figure 4 and plots σ_f^* versus $\dot{\sigma}$ using equation (2). Note that the σ_f^* and $\dot{\sigma}$ scales are logarithmic. The difference in data fit between the exponential and the power-law formulations was minimal, as can be seen by the correlation coefficients in table I or by comparing figures 4 and 5. However, a notable exception to this difference was found for 96-wt% alumina, for which the power-law formulation yielded a better result in data fit compared with the exponential formulation.

Since the SCG parameter n in the power-law formulation is and has been used as an important measure of the SCG susceptibility of brittle materials, it is worthwhile to establish a relationship of n in the exponential formulation with respect to that in the power-law formulation using the data in table I. Figure 6 shows the resulting plots of SCG parameters n for the two formulations. Notwithstanding some variation, there seems to exist a reasonable relationship between the two formulations as approximated in the following relation:^b

$$n_e = 0.9642n_p + 12.5241 \quad (20)$$

with a correlation coefficient of $r^2 = 0.9511$. The n_e and n_p represent SCG parameter n in the exponential and the power-law formulations, respectively. By a rule of thumb, it can be stated that n_e is greater than n_p by approximately 10.

The parameter A can be determined for the exponential and power-law formulations using equation (18) and the B expression of equation (3), respectively. The initial crack size or the critical crack size in the inert condition a_i can be estimated using the basic relation $K_{IC} = Y S_i a_i^{1/2}$, assuming the crack configuration to be a semicircle and the crack size to be small compared with that of the components or test coupons (i.e., an infinite-body approach). The resulting A parameters for each material estimated for both the exponential and power-law formulations are shown in table II. Unlike SCG parameter n , there was no definite relationship in A between the two formulations. However, the actual crack velocities at

^a The ASTM test standards (C1368 and C1465) on constant stress rate testing recommend the use of each individual strength value and the corresponding stress rate in regression analysis to evaluate the SCG parameters. However, for a better representation of data fit, the arithmetic mean value of individual strengths obtained at a given averaged stress rate was used in this work for both plots and SCG parameter estimations. A previous study (ref. 21) showed that the difference in SCG parameters for the individual data method and the arithmetic mean method was negligible.

^b The AS800 silicon nitride exhibited an extraordinarily high SCG resistance with $n \geq 200$ so that the AS800 data were excluded in the plot for a better representation of the remaining ordinary SCG data that are typically in the range of $n = 10$ to 100.

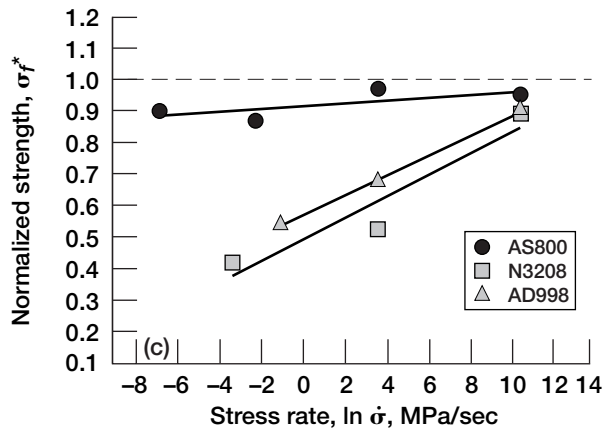
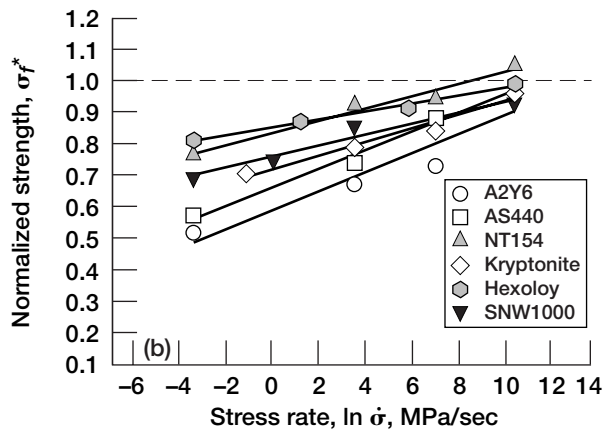
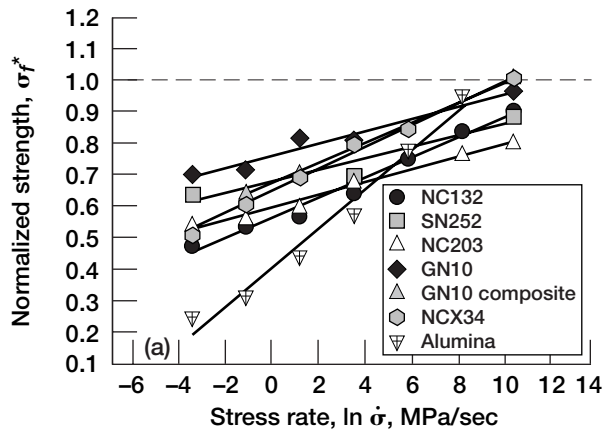


Figure 4.—Normalized strength σ_f^* as function of stress rate $\dot{\sigma}$ in exponential crack-velocity formulation using equation (16) under constant stress rate loading at elevated temperatures in air. (a) NC132, SN252, GN10, and NCX34 silicon nitrides; GN10 composite ($\text{SiC}_w/\text{Si}_3\text{N}_4$); NC203 silicon carbide; 96-wt% alumina. (b) A2Y6, AS440, NT154, and SNW1000 silicon nitrides; Kryptonite $\text{SiC}_w/\text{Si}_3\text{N}_4$; Hexoloy silicon carbide. (c) AS800 and N3208 silicon nitrides; AD998 alumina.

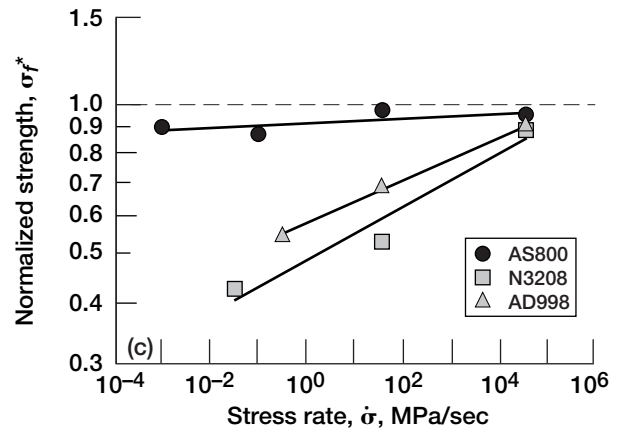
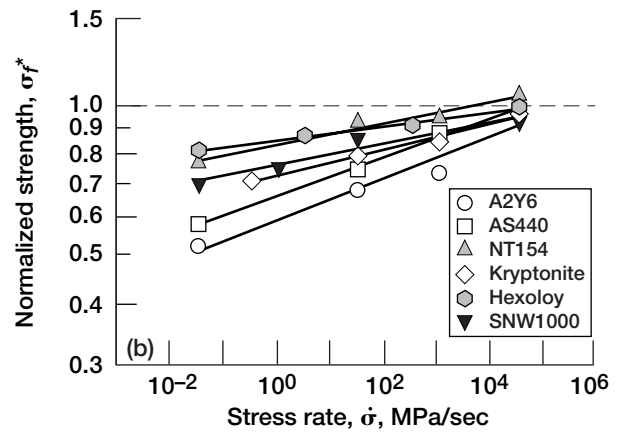
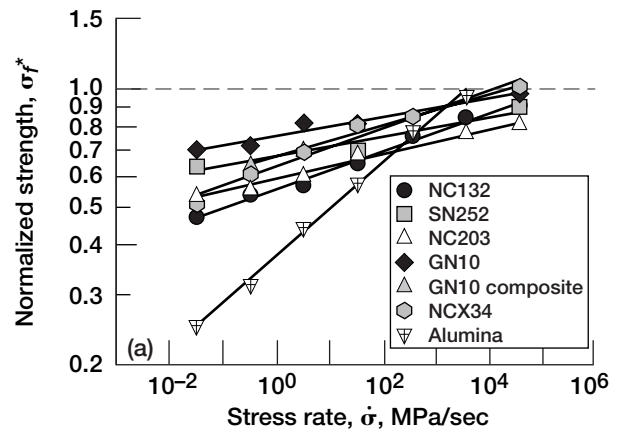


Figure 5.—Normalized strength σ_f^* as function of stress rate $\dot{\sigma}$ in power-law crack-velocity formulation using equation (2) under constant stress rate loading at elevated temperatures in air. (a) NC132, SN252, GN10, and NCX34 silicon nitrides; GN10 composite ($\text{SiC}_w/\text{Si}_3\text{N}_4$); NC203 silicon carbide; 96-wt% alumina. (b) A2Y6, AS440, NT154, and SNW1000 silicon nitrides; Kryptonite $\text{SiC}_w/\text{Si}_3\text{N}_4$; Hexoloy silicon carbide. (c) AS800 and N3208 silicon nitrides; AD998 alumina.

TABLE I.—SUMMARY OF SLOW-CRACK-GROWTH (SCG) PARAMETERS AND CORRELATION COEFFICIENTS OF DATA FIT FOR VARIOUS BRITTLE MATERIALS USING EXPONENTIAL AND POWER-LAW CRACK-VELOCITY FORMULATIONS

[Test methods typically were in accordance with ASTM C1368, C1465, and C1211 (in four-point flexure). Number of specimens tested at each stress rate varied typically from 5 to 10 up to 20 to 30 depending on type of material used.]

| Material ^a | Test conditions | | Formulation | | | | | | Reference |
|--|-----------------|------------------------|------------------------------------|---|------------------------------------|--------------------------------------|--|--------|-----------|
| | Temperature, °C | Number of stress rates | Exponential | | Power law | | Correlation coefficient, ^d r^2 | | |
| | | | SCG parameter, ^b n | SCG parameter, ^{b,c} χ | SCG parameter, ^b n | SCG parameter, ^{b,c} D | | | |
| Pyroceram 96-wt% Al ₂ O ₃ Glass (indented, annealed) | Ambient | 6 | 36.7 | 0.6344 | 0.9957 | 20.1 | 189.8 | 0.9959 | 18 |
| | Ambient | 7 | 61.2 | .7599 | .9832 | 46.8 | 223.2 | .9903 | 19 |
| | Ambient | 5 | 29.2 | .6582 | .9558 | 19.1 | 91.0 | .9658 | 20 |
| 96-wt% Al ₂ O ₃ NC132 Si ₃ N ₄ SN252 Si ₃ N ₄ NC203 SiC GN10 Si ₃ N ₄ GN10 Si ₃ N ₄ composite ^f | 1000 | 5 | 27.5 | .3818 | .9562 | 8.3 | 124.4 | .9933 | 21 |
| | 1100 | 7 | 31.2 | .5579 | .9805 | 19.8 | 562.0 | .9890 | 22 |
| | 1371 | 3 | 55.3 | .6755 | .9150 | 40.7 | 435.8 | .9328 | |
| | 1300 | 6 | 49.4 | .5915 | .9811 | 31.5 | 385.2 | .9785 | |
| | 1300 | 5 | 52.2 | .7591 | .9552 | 42.1 | 553.6 | .9489 | |
| 1300 | 5 | 31.4 | .6702 | .9968 | 24.6 | 468.9 | .9904 | | |
| NCX34 Si ₃ N ₄ 96-wt% Al ₂ O ₃ A2Y6 Si ₃ N ₄ AS440 Si ₃ N ₄ NT154 Si ₃ N ₄ | 1200 | 6 | 28.4 | .6421 | .9915 | 19.8 | 508.7 | .9964 | 22 |
| | 1000 | 6 | 16.1 | .4052 | .9744 | 7.4 | 128.7 | .9964 | |
| | 1200 | 4 | 33.4 | .5919 | .9843 | 22.6 | 410.8 | .9459 | |
| | 1100 | 4 | 33.9 | .6661 | .9890 | 24.6 | 508.1 | .9951 | |
| | 1200 | 4 | 52.3 | .8370 | .9668 | 45.8 | 660.8 | .9681 | |
| Kryptonite ^f Hexoloy SiC SNW1000 Si ₃ N ₄ AS800 Si ₃ N ₄ N3208 Si ₃ N ₄ AD998 Al ₂ O ₃ | 1200 | 4 | 46.7 | .7187 | .9634 | 37.5 | 480.7 | .9782 | 22 |
| | 1371 | 4 | 81.1 | .8538 | .9885 | 71.8 | 285.7 | .9922 | |
| | 1300 | 4 | 58.0 | .7629 | .9479 | 46.0 | 514.9 | .9370 | |
| | 1200 | 4 | 230.0 | .9174 | .538 | 211.0 | 604.0 | .5021 | |
| | 1100 | 3 | 29.3 | .4932 | .9056 | 17.4 | 457.5 | .9462 | |
| | 1000 | 3 | 31.8 | .5710 | .9996 | 21.6 | 173.0 | .9974 | 20 |

^aPyroceram (glass ceramic), Corning, Corning, NY; NC132 and NT154, Norton Advanced Ceramics, Northboro, MA; SN252, Kyocera Corp., Japan; NC203 and NCX34, Norton Co., Worcester, MA; GN10, GN10 composite, and AS800, AlliedSignal, Torrance, CA; A2Y6 and SNW1000, GTE Laboratories, Waltham, MA; AS440, AlliedSignal, Morristown, NJ; Kryptonite, Japan Metals & Chemicals Co., Japan; Hexoloy, Saint-Gobain Advanced Ceramics, Niagara Falls, NY; N3208, Bayer-CFI, Germany; AD998, Coors, Golden, CO.

^bInert strength listed in table II was used in calculating n , χ , and D .

^cParameters D and χ were determined with units of strength in megapascals and stress rate in megapascals per second.

^d r^2 indicates square of correlation coefficient.

^eReference 22 represents results of previous work compiled from various SCG and ultrafast fracture testing experiments.

^fGN10 Si₃N₄ composite and Kryptonite are SiC_w/Si₃N₄ composites.

TABLE II.—SUMMARY OF SLOW-CRACK-GROWTH (SCG) PARAMETER *A* FOR VARIOUS BRITTLE MATERIALS USING EXPONENTIAL AND POWER-LAW CRACK-VELOCITY FORMULATIONS
[Data were obtained from previous experimental work (refs. 18 to 22).]

| Material | Test temperature, °C | Fracture toughness, ^a K_{IC} , Mpa m ^{1/2} | Inert strength, ^b S_i , MPa | SCG parameter <i>A</i> , m/s | |
|---|-------------------------|--|--|---------------------------------|-----------------------|
| | | | | Formulation | |
| | | | | Exponential | Power law |
| Pyroceram (glass ceramic) | Ambient | 2.4 | 303 | 3.04×10^{-17} | 0.01 |
| 96-wt% Al ₂ O ₃ | Ambient | 3.4 | 295 | 5.23×10^{-27} | .47 |
| Glass (indented, annealed) | Ambient | .7 | 140 | 1.79×10^{-15} | .01 |
| 96 wt% Al ₂ O ₃ | 1000 | 3.4 | 344 | 1.78×10^{-11} | 1.87×10^{-3} |
| NC132 Si ₃ N ₄ | 1100 | 4.6 | 1018 | 1.18×10^{-15} | .01 |
| SN252 Si ₃ N ₄ | 1371 | 7.4 | 648 | 2.29×10^{-23} | 5.15 |
| NC203 SiC | 1300 | 4.0 | 655 | 2.23×10^{-20} | 3.16 |
| GN10 Si ₃ N ₄ | 1300 | 5.2 | 732 | 8.16×10^{-25} | .02 |
| GN10 Si ₃ N ₄ composite ^c | 1300 | 5.2 | 698 | 1.29×10^{-16} | 3.70×10^{-3} |
| NCX34 Si ₃ N ₄ | 1200 | 6.9 | 805 | 2.41×10^{-15} | 2.36×10^{-3} |
| 96 wt% Al ₂ O ₃ | 1000 | 3.4 | 344 | 1.14×10^{-9} | 2.61×10^{-3} |
| A2Y6 Si ₃ N ₄ | 1200 | 7.3 | 701 | 8.68×10^{-16} | .08 |
| AS440 Si ₃ N ₄ | 1100 | 7.3 | 773 | 3.73×10^{-17} | .01 |
| NT154 Si ₃ N ₄ | 1200 | 5.5 | 793 | 1.10×10^{-26} | 5.13×10^{-4} |
| Kryptonite ^c | 1200 | 6.6 | 667 | 7.45×10^{-22} | .08 |
| Hexoloy ^d SiC | 1371 | 2.4 | 335 | 2.23×10^{-37} | .03 |
| SNW1000 Si ₃ N ₄ | 1300 | 6.3 | 678 | 1.47×10^{-26} | .09 |
| AS800 Si ₃ N ₄ | 1200 | 7.2 | 659 | 4.39×10^{-99} | 1.00×10^{-4} |
| N3208 Si ₃ N ₄ | 1100 | 5.3 | 951 | 3.90×10^{-14} | .04 |
| AD998 Al ₂ O ₃ | 1000 | 4.7 | 303 | 2.21×10^{-14} | .45 |

^aSEPB (single edge precracked beam) technique was used in fracture toughness evaluation in accordance with ASTM C1421.

^bInert strength was determined in four-point flexure at ambient temperature in oil for SCG-susceptible materials (glass, glass ceramic, and alumina) and in air for SCG-insensitive materials (including most silicon nitrides and silicon carbides). Previous studies on ultrafast strength behavior of various advanced ceramics at elevated temperatures showed that strength at ultrafast test rates of 10^4 to 10^5 MPa/s converged and was close to ambient-temperature inert counterparts (e.g., ref. 22). Consequently, as close approximation, room-temperature inert strength was used as elevated-temperature inert strength in evaluating parameter *A*.

^cGN10 Si₃N₄ composite and Kryptonite (JMC New Materials, Inc., Japan) are SiC_w/Si₃N₄ composites.

^dSaint-Gobain Advanced Ceramics, Niagara Falls, NY.

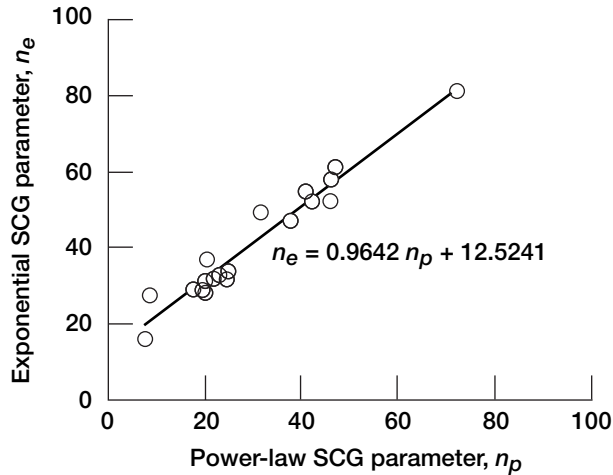


Figure 6.—Relationship in SCG parameters n for materials from table I (excluding AS800) between exponential n_e and power-law n_p crack-velocity formulations.

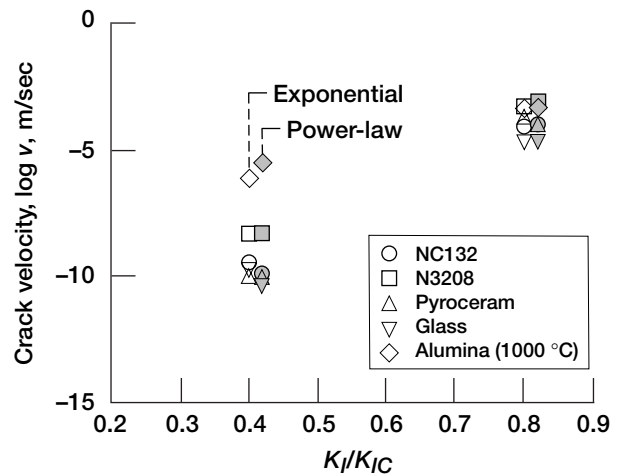


Figure 7.—Typical examples of crack velocity v as function of stress intensity factor K_I/K_{IC} in exponential and power-law formulations for silicon nitrides NC132 and N3208, glass ceramic Pyroceram, soda-lime glass, and 96-wt% alumina (at 1000 °C).

a given stress intensity factor for each formulation seem to be similar, as can be seen from some typical examples in figure 7. Each crack velocity for a given K_I/K_{IC} was calculated using A and n from its respective crack-velocity formula, equation (4) for the exponential formulation, and equation (1) for the power-law formulation.

Preload Analysis and Data

To save test time, a certain amount of preload can be applied to the test specimen quickly prior to testing (see fig. 8) as long as the strength with preload does not differ from the strength with zero preload. A preloading or accelerated testing technique has previously been developed to save test time in constant stress rate testing at both ambient and elevated temperatures (refs. 23 and 24). The solutions, based on the power-law crack-velocity formulation, had been verified by constant stress rate testing using a variety of materials such as glass, glass ceramic, aluminas, silicon carbides, and silicon nitrides at ambient and elevated temperatures. This accelerated test technique has also been adopted in ASTM test standards C1368 and C1468 for constant stress rate testing for advanced ceramics. The resulting equation of strength as a function of preload is expressed as (refs. 23 and 24)

$$\sigma_{pr}^* = \left(1 + \alpha_{pr}^{n+1}\right)^{1/n+1} \quad (21)$$

where σ_{pr}^* is the normalized preload strength in which fatigue strength with preload is normalized with respect to fatigue strength with zero preload, and α_{pr} is the preloading factor ($0 \leq \alpha_{pr} \leq 1$) in which applied preload stress is normalized with respect to fatigue strength with zero preload. Note that equation (21) is valid for a given n regardless of applied stress rate. The resulting plots of equation (21) for various values of n are shown in figure 9. For most glass and advanced ceramics, the values of n are typically ≥ 20 . In this case, the application of a preload corresponding to 90 percent ($\alpha_{pr} = 0.9$) of zero-preload strength results in a maximum strength increase of only 0.5 percent ($\sigma_{pr}^* \leq 1.005$). This 90-percent preload gives rise to a 90-percent savings in test time, which illustrates the dramatic savings of

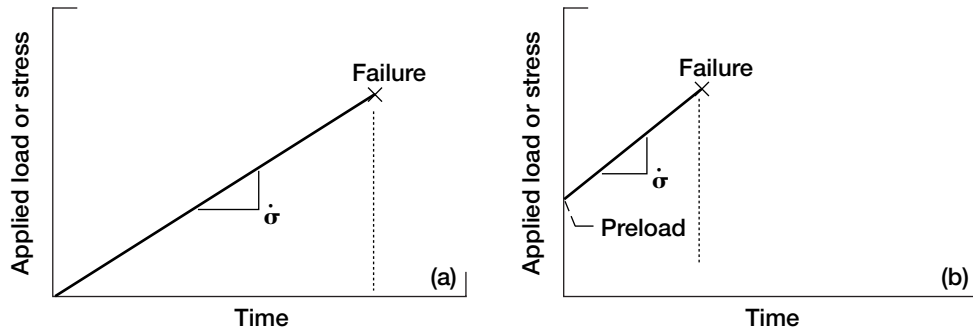


Figure 8.—Modes of loading applied in constant stress rate testing. (a) No preload (conventional testing). (b) Preload (developed, accelerated testing).

test time as a result of preloading. Likewise, an 80-percent preload gives an 80-percent savings in test time with a strength difference of only 0.04 percent ($\sigma_{pr}^* = 1.0004$), and this trend continues. Detailed analysis, experiments, and other important features regarding the preloading technique can be found elsewhere (refs. 18 and 23 to 26).

Similar to the results shown in figure 9, normalized preload strength as a function of preload was determined for the exponential formulation. Because of the typical functional complexity of the exponential formulation, no closed-form solution similar to equation (21) was available other than a numerical solution. The solution of strength as a function of preload was determined at two or three different stress rates for a given SCG parameter n . The values of n ranged from 10 to 70. The stress rates for a given n were chosen such that the corresponding strengths were about 90 percent (for higher stress rates) and 30 to 50 percent (for lower stress rates) of inert strength based on the previous SCG analysis (such as fig. 1) in constant stress rate loading. The results of the preloading analysis for the exponential formulation showed that contrary to the case for the power-law formulation (fig. 9), the normalized preload strength for a given n depends not only on preload but also on stress rate. For a given n , the normalized preload strength increased with decreasing applied stress rate, presumably attributed to the augmented SCG. For higher values of $n \geq 30$, such a normalized preload strength dependency on stress rate became negligible. Hence, the use of normalized preload strength determined at lower stress rates would be preferred for a conservative estimation as well as for simplicity.

The resulting plots thus simplified are shown in figure 10. For example, a preload corresponding to 90 percent ($\alpha_p = 0.9$) of zero-preload strength, which is a maximum preload that can be applied to a few materials in actual testing, results in a strength increase of 3.5, 1.7, 1.1, 0.5, 0.3, and 0.1 percent for $n = 20, 30, 40, 50, 60,$ and 70 , respectively. In comparison, the power-law formulation results in strength increases of 2.5, 0.5, 0.1, and ≤ 0.03 percent for $n = 10, 20, 30,$ and ≥ 40 , respectively. Note that the n values used in this comparison were approximately equivalent to each other based on the relation of equation (20). Therefore, compared with the power-law counterpart, the exponential formulation slightly overestimates preload strength, particularly for lower values of $n < 30$. For the case of $n \geq 30$, the difference in normalized preload strength between the power-law and exponential formulations is practically insignificant.

As mentioned in the foregoing preload analysis, the difference in normalized preload strength between the two formulations was negligible for $n \geq 30$ whereas the difference was amplified for $n \leq 20$. Hence, the verification of the preload analysis would be evident if data from a material showing significant susceptibility to SCG, $n < 20$, are used. This is the case for 96-wt% alumina tested at 1000 °C in air (ref. 24). This material exhibited an extraordinary SCG susceptibility with $n = 16.1$ and 7.4 for the exponential and power-law formulations, respectively, as seen in table I and figures 4 and 5. Figure 11 depicts the results of fracture stress as a function of preload for 96-wt% alumina determined at stress rates of 0.333 and 0.033 MPa/s (ref. 24). The exact solution (theoretical prediction) of strength as a function of preload was also included for both the exponential and power-law formulations. As seen from the figure,

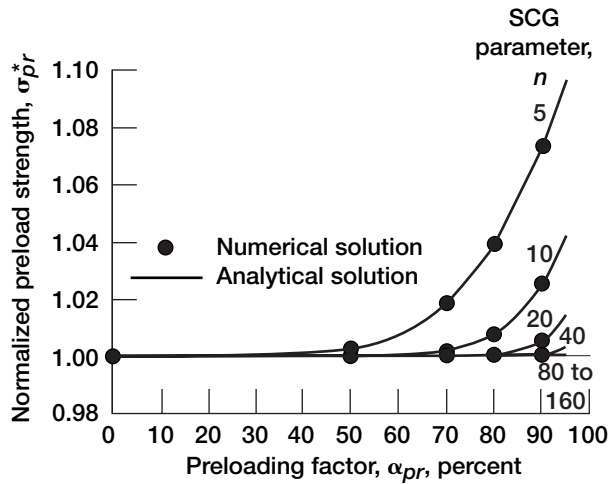


Figure 9.—Normalized preload strength σ_{pr}^* as function of preloading factor α_{pr} for various values of SCG parameter n in power-law crack-velocity formulation (ref. 23).

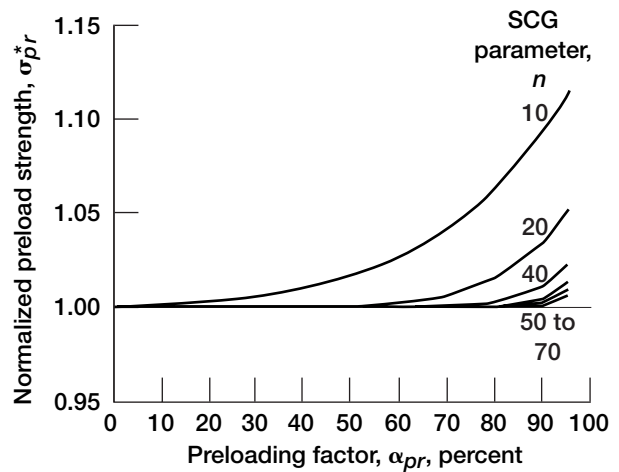


Figure 10.—Normalized preload strength σ_{pr}^* as function of preloading factor α_{pr} for various values of SCG parameter n in exponential crack-velocity formulation.

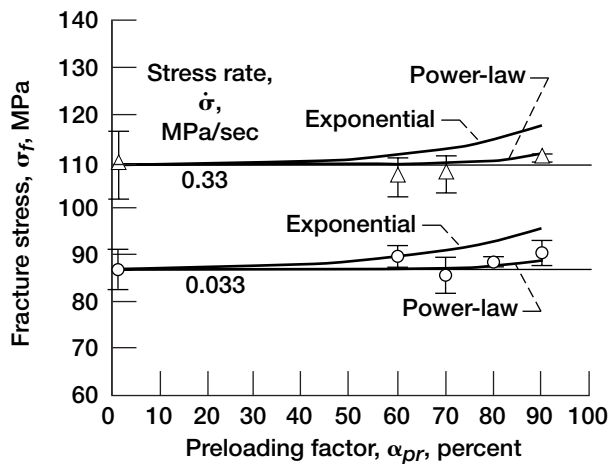


Figure 11.—Comparison of preload data for 96-wt% alumina (ref. 24) and theoretical predictions based on exponential and power-law crack-velocity formulations.

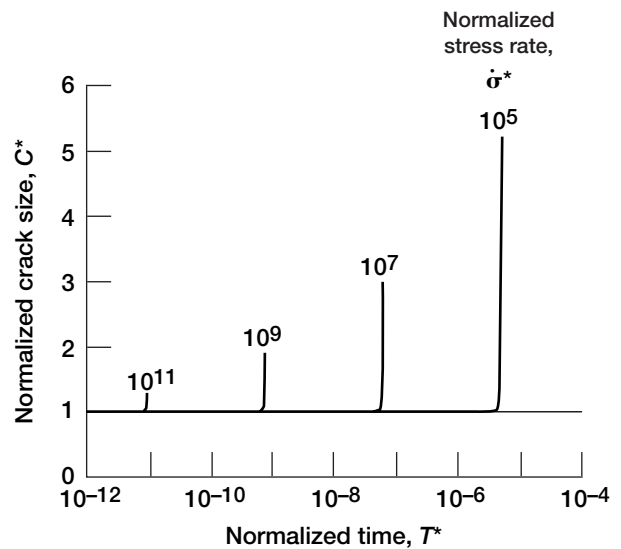


Figure 12.—Typical examples of crack growth as function of time for different stress rates $\dot{\sigma}^*$ in constant stress rate testing for SCG parameter $n = 30$ in exponential crack-velocity formulation.

the power-law prediction is in far better agreement with the data than the exponential formulation at either 0.33 or 0.03 MPa/s. The predicted strength increases at $\alpha_{pr} = 0.9$ were about 8 and 4 percent, respectively, for the exponential and power-law formulations. This preload result indicates that the overall slow-crack-growth behavior of a material can be better described by the power-law crack velocity, noting again that the preload analysis is simply an extension of the general SCG analysis using a particular crack-velocity form. As a consequence, the preloading technique can be used not only as a time-saving technique during testing but also as a tool in validating the appropriateness of a crack-velocity form used in life prediction analysis. Recently, the preloading technique has been used to pinpoint possible governing failure mechanisms of various ceramic matrix composites tested in tension at elevated temperatures (ref. 27).

The applicability of the preloading technique in the power-law formulation is attributed to the long incubation time of an initial crack, typical of most brittle materials with $n \geq 20$ (ref. 23). In other words, the initial crack starts to grow at close to failure time after a long incubation time. Figure 12 shows a typical example of crack growth as a function of time during constant stress rate testing for $n = 30$ at four stress rates ($\dot{\sigma}^* = 10^5, 10^7, 10^9, \text{ and } 10^{11}$) in the exponential formulation. The crack growth, regardless of stress rate, is exemplified by the unique feature that most of crack growth takes place very close to failure and results from the long incubation time of an initial crack. Hence, the unique feature of a long incubation time for an initial crack is thus equally characterized for both the exponential and power-law SCG formulations. This feature is the reason why the difference in normalized preload strength as a function of preload between the two formulations diminished with increasing SCG resistance for the case of $n \geq 30$.

Conclusions

Based on the comparison of exponential and power-law formulation analyses of the slow crack growth (SCG) of selected ceramics under constant stress rate loading, the following conclusions were made:

1. The data fit to the relation strength as a function of stress rate (σ_f versus $\ln \dot{\sigma}$) in the exponential crack-velocity formulation was very reasonable for most of the materials studied. The most notable exception was 96-wt% alumina at elevated temperature. However, one has to know the inert strength of a material a priori to evaluate the important SCG parameter n , whereas in the power-law formulation inert strength need not be known.
2. The preloading technique was equally applicable in both formulations for the case of $n > 30$. However, for the lower n value of $n < 20$, in which significant SCG occurs, the preload data were not in good agreement with the theoretical prediction in the exponential formulation as compared with the power-law formulation.
3. The data fit and applicability of the preloading technique for $n > 30$ were similar for both formulations. However, a priori knowledge of the inert strength of a material to evaluate the SCG parameter n is a requirement of the exponential formulation. Also, the exponential formulation involves a more complex analysis not only for the estimation of SCG parameters but also for the life prediction of structural components. These attributes make the power-law formulation a far more preferable choice than the exponential formulation for analysis during constant stress rate loading.

Appendix—Symbols

| | |
|----------------|--|
| <i>A</i> | slow-crack-growth parameter defined in equations (1) and (4) |
| <i>a</i> | crack size |
| <i>B</i> | slow-crack-growth parameter, $B = 2K_{IC} / [AY^2(n - 2)]$ |
| <i>C</i> | crack size in the normalized scheme of references 15 and 16 |
| <i>D</i> | slow-crack-growth parameter defined in equation (3) |
| <i>K</i> | stress intensity factor |
| <i>n</i> | slow-crack-growth parameter defined in equations (1) and (4) |
| r^2 | correlation coefficient |
| <i>S</i> | strength |
| <i>T</i> | time in the normalized scheme of references 15 and 16 |
| <i>t</i> | time |
| <i>v</i> | crack velocity |
| <i>Y</i> | crack geometry factor |
| α | factor from equation (21) |
| β | intercept of curve in linear regression analysis equation (12) |
| σ | applied stress |
| $\dot{\sigma}$ | applied stress rate |
| χ | slow-crack-growth parameter defined in equation (18) |

Subscripts:

| | |
|----------|-------------------------|
| <i>C</i> | critical |
| <i>e</i> | exponential formulation |
| <i>f</i> | fracture |
| <i>I</i> | mode I |

i inert or initial condition

p power-law formulation

pr preload

Superscripts:

* normalized

' apparent (calculated)

References

1. Standard Test Method for Determination of Slow Crack Growth Parameters of Advanced Ceramics by Constant Stress-Rate Flexural Testing at Ambient Temperature. Annual Book of ASTM Standards 2001, ASTM Designation: C 1368-00, sec. 15, vol. 15.01, ASTM, West Conshohocken, PA, 2001, pp. 626-634.
2. Standard Test Method for Determination of Slow Crack Growth Parameters of Advanced Ceramics by Constant Stress-Rate Flexural Testing at Elevated Temperatures. Annual Book of ASTM Standards 2001, ASTM Designation: C 1465-00, sec. 15, vol. 15.01, ASTM, West Conshohocken, PA, 2001, pp. 703-716.
3. Choi, S.R.; Nemeth, N.N.; and Gyekenyesi, J.P.: Slow Crack Growth of Brittle Materials With Exponential Crack Velocity Formulation—Part 1: Analysis. NASA/TM—2002-211153-1.
4. Evans, A.G.: Slow Crack Growth in Brittle Materials Under Dynamic Loading Conditions. *Int. J. Fracture*, vol. 10, no. 2, 1974, pp. 251-259.
5. Ritter, John E., Jr.: Engineering Design and Fatigue Failure of Brittle Materials. *Fracture Mechanics of Ceramics*, R.C. Bradt, D.P.H. Hasselman, and F.F. Lange, eds., vol. 4, Plenum Press, New York, NY, 1978, pp. 667-686.
6. Hillig, W.B.; and Charles, R.J.: Surfaces, Stress-Dependent Surface Reactions, and Strength. *High Strength Materials*, Victor F. Zackay, ed., ch. 17, John Wiley & Sons, Inc., New York, NY, 1965, 682-705.
7. Charles, R.J.: Diffusion Controlled Stress Rupture of Polycrystalline Materials. *Metall. Trans. A*, vol. 7A, no. 8, 1976, pp. 1081-1089.
8. Pollet, J.-C.; and Burns, S.J.: Thermally Activated Crack Propagation—Theory. *Int. J. Fracture*, vol. 13, no. 5, 1977, pp. 667-679.
9. Wiederhorn, S.M.; and Bolz, L.H.: Stress Corrosion and Static Fatigue of Glass. *J. Am. Ceram. Soc.*, vol. 53, no. 10, 1970, pp. 543-548.
10. Lawn, B.R.: An Atomistic Model of Kinetic Crack Growth in Brittle Solids. *J. Mater. Sci.*, vol. 10, 1975, pp. 469-480.
11. Lenoë, E.M.; and Neal, D.M.: Assessment of Strength-Probability-Time Relationships in Ceramics. ARPA Order 2181, AMMRC-TR-75-13, 1975.
12. Trantina, G.G.: Strength and Life Prediction for Hot-Pressed Silicon Nitride. *J. Am. Cer. Soc.*, vol. 62, no. 7-8, 1979, pp. 377-380.
13. Ritter, John E., et al.: Dynamic Fatigue Analysis of Indentation Flaws Using an Exponential-Law Crack Velocity Function. *Commun. Am. Ceram. Soc.*, 1984, pp. C-198—C-199.
14. Ritter, John E., Jr.; Jakus, Karl; and Cooke, David S.: Predicting Failure of Optical Glass Fibers. *Proceedings of Second International Conference on Environmental Degradation of Engineering Materials*, 1981, pp. 565-575.
15. Lawn, B.R., et al.: Fatigue Analysis of Brittle Materials Using Indentation Flaws. *J. Mat. Sci.*, pt. 1, vol. 16, no. 10, 1981, pp. 2846-2854.
16. Choi, S.R.; Ritter, J.E.; and Jakus, K.: Failure of Glass With Subthreshold Flaws. *J. Am. Ceram. Soc.*, vol. 73, no. 2, 1990, pp. 268-274.
17. Choi, Sung R.; Salem, Jonathan A.; and Holland, Frederic A.: Estimation of Slow Crack Growth Parameters for Constant Stress-Rate Test Data of Advanced Ceramics and Glass by the Individual Data and Arithmetic Mean Methods. NASA TM-107369, 1997. <http://gltrs.grc.nasa.gov/GLTRS> Accessed Jan. 16, 2002.

18. Choi, Sung R., et al.: Accelerated Testing Methodology in Constant Stress-Rate Testing for Advanced Structural Ceramics—A Preloading Technique. ASME 2001-GT-460, 2001.
19. Choi, Sung R.; Powers, Lynn M.; and Nemeth, Noel N.: Slow Crack Growth Behavior and Life/Reliability Analysis of 96 wt% Alumina at Ambient Temperature With Various Specimen/Loading Configurations. NASA/TM—2000-210206, 2000. <http://gltrs.grc.nasa.gov/GLTRS> Accessed Jan. 16, 2002.
20. Choi, S.R.; and Gyekenyesi, J.P.: Slow Crack Growth Analysis of Brittle Materials With Finite Thickness Subjected to Constant Stress-Rate Flexural Loading. *J. Mater. Sci.*, vol. 34, no. 16, 1999, pp. 3875–3882.
21. Choi, Sung R.: Specimen Geometry Effect on the Determination of Slow Crack Growth Parameters of Advanced Ceramics in Constant Flexural Stress-Rate Testing at Elevated Temperatures. *Ceramic Engineering & Science Proceedings*, vol. 20, issue 3, American Ceramic Society, Westerville, OH, 1999, pp. 525–534.
22. Choi, Sung R.; and Gyekenyesi, John P.: “Ultra”-Fast Fracture Strength of Advanced Structural Ceramics at Elevated Temperatures: An Approach to High-Temperature ‘Inert’ Strength. *Fracture Mechanics of Ceramics*, R.C. Bradt et al., eds., Vol. 13, Kluwer Academic/Plenum Publishers, New York, NY, 2002, pp. 27–46.
23. Choi, S.R.; and Gyekenyesi, J.P.: Fatigue Strength as a Function of Preloading in Dynamic Fatigue Testing of Glass and Ceramics. *J. Eng. Gas Turbines Power*, vol. 119, 1997, pp. 493–499.
24. Choi, Sung R.; and Salem, Jonathan A.: Effect of Preloading on Fatigue Strength in Dynamic Fatigue Testing of Ceramic Materials at Elevated Temperatures. *Ceramic Engineering & Science Proceedings*, American Ceramic Society, Westerville, OH, 1995, pp. 87–94.
25. Choi, Sung R.; and Salem, Jonathan A.: Preloading Technique in Dynamic Fatigue Testing of Glass and Ceramics With an Indentation Flaw System. *J. Am. Ceram. Soc.*, vol. 79, no. 5, 1996, pp. 1228–1232.
26. Choi, S.R.; and Salem, J.A.: Preloading Technique in Dynamic Fatigue Testing of Ceramics: Effect of Preloading on Strength Variation. *J. Mater. Sci. Lett.*, vol. 15, 1996, pp. 1963–1965.
27. Choi, Sung R.; and Gyekenyesi, John P.: Effect of Load Rate on Tensile Strength of Various CFCC’s at Elevated Temperatures—An Approach to Life Prediction Testing. *Ceramic Engineering & Science Proceedings*, vol. 22, issue 3, 2001, pp. 597–606.

REPORT DOCUMENTATION PAGE

Form Approved
OMB No. 0704-0188

Public reporting burden for this collection of information is estimated to average 1 hour per response, including the time for reviewing instructions, searching existing data sources, gathering and maintaining the data needed, and completing and reviewing the collection of information. Send comments regarding this burden estimate or any other aspect of this collection of information, including suggestions for reducing this burden, to Washington Headquarters Services, Directorate for Information Operations and Reports, 1215 Jefferson Davis Highway, Suite 1204, Arlington, VA 22202-4302, and to the Office of Management and Budget, Paperwork Reduction Project (0704-0188), Washington, DC 20503.

| | | | |
|--|---|--|-----------------------------------|
| 1. AGENCY USE ONLY (<i>Leave blank</i>) | 2. REPORT DATE June 2002 | 3. REPORT TYPE AND DATES COVERED Technical Memorandum | |
| 4. TITLE AND SUBTITLE Slow Crack Growth of Brittle Materials With Exponential Crack-Velocity Formulation—Part 2: Constant Stress Rate Experiments | | 5. FUNDING NUMBERS WU-708-31-13-00 | |
| 6. AUTHOR(S) Sung R. Choi, Noel N. Nemeth, and John P. Gyekenyesi | | | |
| 7. PERFORMING ORGANIZATION NAME(S) AND ADDRESS(ES) National Aeronautics and Space Administration John H. Glenn Research Center at Lewis Field Cleveland, Ohio 44135-3191 | | 8. PERFORMING ORGANIZATION REPORT NUMBER E-13009-2 | |
| 9. SPONSORING/MONITORING AGENCY NAME(S) AND ADDRESS(ES) National Aeronautics and Space Administration Washington, DC 20546-0001 | | 10. SPONSORING/MONITORING AGENCY REPORT NUMBER NASA TM-2002-211153-PART2 | |
| 11. SUPPLEMENTARY NOTES Sung R. Choi, Ohio Aerospace Institute, Brook Park, Ohio 44142; Noel N. Nemeth and John P. Gyekenyesi, NASA Glenn Research Center. Responsible person, Sung R. Choi, organization code 5920, 216-433-8366. | | | |
| 12a. DISTRIBUTION/AVAILABILITY STATEMENT Unclassified - Unlimited Subject Categories: 07 and 39 Available electronically at http://gltrs.grc.nasa.gov/GLTRS This publication is available from the NASA Center for AeroSpace Information, 301-621-0390. | | 12b. DISTRIBUTION CODE | |
| 13. ABSTRACT (<i>Maximum 200 words</i>) The previously determined life prediction analysis based on an exponential crack-velocity formulation was examined using a variety of experimental data on glass and advanced structural ceramics in constant stress rate and preload testing at ambient and elevated temperatures. The data fit to the relation of strength versus the log of the stress rate was very reasonable for most of the materials. Also, the preloading technique was determined equally applicable to the case of slow-crack-growth (SCG) parameter $n > 30$ for both the power-law and exponential formulations. The major limitation in the exponential crack-velocity formulation, however, was that the inert strength of a material must be known a priori to evaluate the important SCG parameter n , a significant drawback as compared with the conventional power-law crack-velocity formulation. | | | |
| 14. SUBJECT TERMS Slow crack growth analysis; Life prediction; Brittle materials; Ceramics and glass; Life prediction testing; Mechanical testing | | 15. NUMBER OF PAGES 26 | |
| | | 16. PRICE CODE | |
| 17. SECURITY CLASSIFICATION OF REPORT Unclassified | 18. SECURITY CLASSIFICATION OF THIS PAGE Unclassified | 19. SECURITY CLASSIFICATION OF ABSTRACT Unclassified | 20. LIMITATION OF ABSTRACT |